Bioactive Materials 6 (2021) 2999–3012

Contents lists available at ScienceDirect

Bioactive Materials

journal homepage: www.sciencedirect.com/journal/bioactive-materials

Cell sheet formation enhances the therapeutic effects of human umbilical cord mesenchymal stem cells on myocardial infarction as a bioactive material

Rui Guo, M.D., Ph.D. [a,b], Feng Wan [a,c], Masatoshi Morimatsu [a,b], Qing Xu [a], Tian Feng [a,d], Hang Yang [a], Yichen Gong [a], Shuhong Ma [a,e], Yun Chang [a,e], Siyao Zhang [a,e], Youxu Jiang [a,e], Heqing Wang [a,c], Dehua Chang [a,f], Hongjia Zhang [a,g], Yunpeng Ling [a,**], Feng Lan [a,e,h,*]

[a] Department of Cardiac Surgery, Peking University Third Hospital, Beijing, 100191, China
[b] Department of Cardiovascular Physiology, Graduate School of Medicine, Dentistry and Pharmaceutical Sciences, Okayama University, Okayama, 700-8558, Japan
[c] Department of Cardiovascular Surgery, Tongji University East Hospital, Shanghai, 200120, China
[d] Department of Neurology, Graduate School of Medicine, Dentistry and Pharmaceutical Sciences, Okayama University, Okayama, 700-8558, Japan
[e] State Key Laboratory of Cardiovascular Disease, Fuwai Hospital, National Center for Cardiovascular Diseases, Chinese Academy of Medical Sciences and Peking Union Medical College, Beijing, 100037, China
[f] Department of Cardiac Surgery, The University of Tokyo Hospital, Tokyo, 113-8655, Japan
[g] Beijing Laboratory for Cardiovascular Precision Medicine, MOE Key Laboratory of Medical Engineering for Cardiovascular Diseases, Anzhen Hospital, Capital Medical University, Beijing, 100029, China
[h] Fuwai Hospital Chinese Academy of Medical Sciences, Shenzhen, Shenzhen, China

ARTICLE INFO

Keywords:
Mesenchymal stem cells
Cell sheet
Myocardial infarction
Regulation of inflammatory response
Ventricular remodelling

ABSTRACT

Stem cell-based therapy has been used to treat ischaemic heart diseases for two decades. However, optimal cell types and transplantation methods remain unclear. This study evaluated the therapeutic effects of human umbilical cord mesenchymal stem cell (hUCMSC) sheet on myocardial infarction (MI).

Methods: hUCMSCs expressing luciferase were generated by lentiviral transduction for *in vivo* bio-luminescent imaging tracking of cells. We applied a temperature-responsive cell culture surface-based method to form the hUCMSC sheet. Cell retention was evaluated using an *in vivo* bio-luminescent imaging tracking system. Unbiased transcriptional profiling of infarcted hearts and further immunohistochemical assessment of monocyte and macrophage subtypes were used to determine the mechanisms underlying the therapeutic effects of the hUCMSC sheet. Echocardiography and pathological analyses of heart sections were performed to evaluate cardiac function, angiogenesis and left ventricular remodelling.

Results: When transplanted to the infarcted mouse hearts, hUCMSC sheet significantly improved the retention and survival compared with cell suspension. At the early stage of MI, hUCMSC sheet modulated inflammation by decreasing Mcp1-positive monocytes and CD68-positive macrophages and increasing Cx3cr1-positive non-classical macrophages, preserving the cardiomyocytes from acute injury. Moreover, the extracellular matrix produced by hUCMSC sheet then served as bioactive scaffold for the host cells to graft and generate new epicardial tissue, providing mechanical support and routes for revascularsation. These effects of hUCMSC sheet treatment significantly improved the cardiac function at days 7 and 28 post-MI.

Conclusions: hUCMSC sheet formation dramatically improved the biological functions of hUCMSCs, mitigating adverse post-MI remodelling by modulating the inflammatory response and providing bioactive scaffold upon transplantation into the heart.

Translational perspective: Due to its excellent availability as well as superior local cellular retention and survival, allogenic transplantation of hUCMSC sheets can more effectively acquire the biological functions of hUCMSCs, such as modulating inflammation and enhancing angiogenesis. Moreover, the hUCMSC sheet method allows the

Peer review under responsibility of KeAi Communications Co., Ltd.
* Corresponding author. Department of Cardiac Surgery, Peking University Third Hospital, Beijing, 100191, China.
** Corresponding author.
E-mail addresses: rui_guo@pku.edu.cn (R. Guo), micsling@pku.edu.cn (Y. Ling), fenglan@pku.edu.cn (F. Lan).

https://doi.org/10.1016/j.bioactmat.2021.01.036
Received 1 November 2020; Received in revised form 21 January 2021; Accepted 28 January 2021

transfer of an intact extracellular matrix without introducing exogenous or synthetic biomaterial, further improving its clinical applicability.

1. Introduction

Coronary artery disease is a major cause of mortality and morbidity in the world [1,2], leading to multiple unfavourable effects, such as heart failure [3,4], myocardial infarction (MI) and adverse ventricular remodelling [5]. MI causes extensive cardiomyocyte death, resulting in a critical intense inflammatory reaction and creating a second lesion on the heart. Without the opportune regulation of the inflammatory response post-MI, the heart eventually undergoes serious problems such as cardiac dysfunction [6].

Medical and surgical treatments for MI can achieve myocardial reperfusion, but cardiomyocyte death due to ischaemia cannot be reversed [7,8].

Stem cell-based regenerative medicine has the potential to treat such irreversible damage to cardiomyocytes caused by ischaemia. In the past two decades, numerous clinical trials on stem cell therapy for ischaemic heart disease have been conducted worldwide [9]. Researchers have tried stem cell transplantation through coronary, venous and myocardial injections but failed to maintain efficient and long-term retention. One clinical trial found that stem cells benefits only existed in the injection site [10]. Therefore, ensuring extensive retention of stem cells in damaged areas of the heart is critical to improving the efficiency of stem cell treatment for ischaemic heart disease.

Currently, stem cells used for the treatment of ischaemic heart disease are mainly mesenchymal stem cells and pluripotent stem cell-derived cardiomyocytes (PSCs-CMs). Clinical application of human embryonic stem cells (hESCs) is limited because of ethical issues. In the case of induced PSCs-CMs, the issue of electrical coupling to the host heart, which might cause post-transplant arrhythmia, remains to be addressed [11,12]. In addition, transplantation of embryonic stem cells or induced pluripotent stem cells derived functional cells suffer from the risk contamination of undifferentiated cells, limiting their clinical application [13]. Therefore, determining a more appropriate stem cell type in the application of clinical patients with heart diseases remains urgent and pivotal in basic and clinical research.

Human mesenchymal stem cells (hMSCs) can be isolated from various types of tissues and can differentiate into mesenchymal and non-mesenchymal tissues *in vitro* and *in vivo* [14]. hMSCs are widely used in the clinical treatment of ischaemic heart disease [9]. Among hMSCs, human umbilical cord mesenchymal stem cells (hUCMSCs) derived from a neonatal organ overcome the drawbacks of adult cells, such as senescence and background diseases [15–17]. For clinical application, hUCMSCs provide advantages of low immunogenicity and better harvest feasibility [18]. A clinical trial showed that hUCMSCs are safe and effective in MI patients [19].

Cell sheet transplantation is a well-established technique that allows sheet formation of adherent cultured cells via cell–cell junctions and physical detachment from the culture dish surface under temperature differential conditions [20–22]. By using a cell sheet, considerably numerous cells can be stably transplanted into the damaged myocardium, depending on the cell sheet size [23–25]. Several animal experiments and clinical trials have demonstrated the feasibility of using cell sheet transplantation to treat ischaemic heart disease [22,26–33]. More importantly, compared with direct stem-cell injection, cell sheet transplantation in MI possesses multiple advantages, including prolonged retention and survival, improved engraftment, functional metabolic environment and better prognosis [34–38].

Transplanted mesenchymal stem cell (MSC)-derived sheets indeed show cardiomyogenesis and dramatic paracrine effects to certain extent. In MI, MSC sheets derived from bone, adipose, menstrual blood and placental tissues contribute to cardioprotection, vascularisation, improved left ventricular function and myocardial repair in various experimental animals; thus, MSC sheets have multiple effects for improving cardiac function in MI [26,27,29,39–44]. More importantly, MSC sheets have lower immunogenicity, extensive clinical safety experience, stronger paracrine ability, more efficient inflammatory regulation, stronger neovascularisation, and no risk of arrhythmia compared with other stem cell-derived sheets [22,37,45]. Therefore, MSC sheets are a more promising approach in MI therapy.

The present study is the first to generate cell sheets from hUCMSCs, evaluate their safety and efficacy, and examine their therapeutic effect mechanisms, including immunoinflammatory regulation and angiogenesis, in an acute myocardial infarction (AMI) mouse model.

2. Methods

2.1. Ethics

All animal procedures were performed in accordance with the animal experimentation guidelines set forth and approved by the Institutional Animal Care and Use Committee (LA2019086) and Peking University Laboratory Animal Welfare Committee and implemented the European Parliament prescriptive Directive 2010/63/EU. All mice were managed and bred in a specific-pathogen-free (SPF) environment. They were administered 1%–5% isoflurane inhalation anaesthesia for surgery and were euthanised using isoflurane with heart excision.

For *in vitro* hUCMSC experiments, umbilical cord donors provided written informed consent. All procedures complied with the Declaration of Helsinki and were approved by the institutional ethics committee (LLPJ2018[001]) of OASIS International Hospital, Beijing, China. The hUCMSC sheet formation procedure was performed according to good manufacturing practices (GMP)-level laboratory provided by the BOE Regenerative Medicine Institute, Beijing, China.

2.2. hUCMSC isolation, characterisation and sheet formation

hUCMSCs were isolated from a caesarean section–wasted umbilical cord obtained from donors. Briefly, well-dissected Wharton's jelly tissue from the umbilical cord was cultured as explants in minimum Essential Medium (MEM) with 10% foetal bovine serum (FBS). The primary hUCMSCs derived were cultured to the fourth passage (P4). Then, hUCMSC marker identification was performed using flow cytometry. P4 hUCMSCs were incubated with antibodies CD73-PE, CD90-FITC, CD105-APC, CD19-FITC, CD34-PE and CD45-APC for 20 min at room temperature, and flow cytometry detection was performed as per the manufacturer's instructions. All flow cytometry antibodies were obtained from Becton, Dickinson and Company (Franklin Lakes, NJ, USA).

To generate an hUCMSC sheet, hUCMSCs cultured to the fifth passage (P5) were planted onto a temperature-responsive cell culture surface (Thermo Fisher Scientific, Waltham, MA, USA), incubated overnight in a 3.5 cm temperature-responsive culture dish at 37 °C and then moved to room temperature for ~40 min. The hUCMSCs formed a sheet automatically. Immunofluorescence staining for fibronectin, β1-integrin and 4',6-diamidino-2-phenylindole (DAPI) staining were performed on cryo-sections of the hUCMSC sheet (For detailed information of antibodies see Supplementary Table 1).

2.3. Luciferase-hUCMSC generation

hUCMSCs were cultured in a 10 cm dish with MEM and 10% FBS until confluence reached 50%–70% and then transfected with lentivirus-expressing luciferase for 5 days. (For detailed information of lentivirus

see Supplementary Fig. 3).

2.4. AMI mouse model and cell transplantation

Surgical induction of MI was performed on 16–18-week-old (body weight 36–42 g) male SPF-level Institute of Cancer Research (ICR) mice the other name Clr:CD-1 and non-obese diabetic/severe combined immune deficiency spontaneous mutation (NOD/SCID) mice as follows:

1. The mice were anesthetised using 3%–5% isoflurane, orotracheally intubated with a light guide and connected to a ventilator, with 1.5%–3% isoflurane for anaesthesia maintenance. The respiratory rate was within 120 times/min, tidal volume 280 μL and airway pressure 10–14 cm water column.
2. The left chest wall was shaved and disinfected. The heart was then exposed via left thoracotomy and ligation of left anterior descending (LAD) coronary artery was performed using a 6-0 non-absorbable suture under a stereoscope (LAD ligation site see Supplementary Fig. 1). The heart was constantly monitored using three unipolar limb lead electrocardiography.
3. The mice were divided into four groups, with 3–16 mice in each group: cell sheet (ICR and NOD/SCID mice), cell suspension, MI-only and control. For the cell sheet group, a wild-type (WT) hUCMSC sheet (~1×10^6 WT hUCMSCs/sheet) and a luciferase-hUCMSC sheet (~5×10^5 luciferase-hUCMSCs and 5×10^5 WT hUCMSCs/sheet) were directly transplanted to the MI area and stabilised for ~3 min. For the cell suspension group, a wild-type (WT) hUCMSC suspension (~1×10^6 WT hUCMSCs/40 μL of Dulbecco's phosphate-buffered saline [DPBS]) and a luciferase-hUCMSC suspension (approximately 5×10^5 luciferase-hUCMSCs and 5×10^5 WT hUCMSCs/40 μL of DPBS), suspended in DPBS, were delivered into the MI and border zones via four intra-myocardial injections. For the MI-only group, no cell sheet or cell suspension was administered. For the control group, a suture was passed around the LAD without ligation.
4. Finally, the open chest was closed

2.5. In vivo bio-luminescent imaging

Mice were anesthetised using 1%–3% isoflurane and oxygen. Xeno-Light D-luciferin (Xenogen Co., Alameda, CA, USA) at a dose of 150 μg/g of body weight was injected intraperitoneally. Images were generated using Xenogen IVIS imaging system (Xenogen Co.). For each mouse, images were obtained at 10–15 min after substrate injection. Xenogen software was used to analyse the images, and the output represented the number of photons emitted/s/cm^2 as a colour image, where red was maximum and blue was minimum. Other bio-luminescent imaging details were determined as previously described [46].

Sections of mouse hearts in the cell sheet group were stained with hematoxylin-eosin and immunostained with anti-human nuclei antigen on post-operative days 1, 5, 9, and 28 (Detailed information of antibodies see Supplementary Table 1). Images were taken under an LSM780 confocal laser microscope (Zeiss, Oberkochen, Germany).

2.6. Transcriptome sequencing and gene ontology biological process analysis

For ICR mice, ischaemic heart injury tissue samples were harvested on post-operative day 5: MI-only, treatment and sham groups: below the ligation point), and the total RNA was isolated using Trizol (Invitrogen, Carlsbad, CA, USA).

Transcriptome libraries were constructed using the NEB Next® Ultra™ RNA Library Prep Kit for Illumina® (New England BioLabs, Ipswich, MA, USA) according to the manufacturer's instructions. The library fragments established were purified using the QIAquick PCR Purification Kit (QIAGEN, Hilden, Germany). A poly(A) tail and adapter were added to the purified complementary DNA (cDNA) via end-joining. Target fragments were retrieved using agarose gel electrophoresis and amplified using polymerase chain reaction (PCR). Quality-qualified libraries passed the quality test and were sequenced using the Illumina Platform (sequencing strategy PE150) to measure messenger RNA (mRNA) expression.

Whole genome gene expression profiling of ICR mice samples was performed using Mus_musculus.GRCm38.91. Thereafter, adapter-polluted reads, low-quality reads and reads containing N >50% were removed to filter high-quality clean reads for subsequent gene expression and Gene Ontology Biological Process (GO:BP) analysis.

The mRNA abundance was quantified using fragments per kilobase per million mapped fragments (FPKM) [47], reflecting the gene expression level.

The DESeq2 package was used for gene differential expression analysis. Differentially expressed genes (DEGs) were selected using $|\log2\text{fold-change}| \geq 1$ and q (P after correction) <0.05. GO:BP analysis was performed on the basis of these DEGs. In addition, inflammation-related biological processes, such as inflammatory response (GO:0006954), negative regulation of inflammatory response (GO:0050728) and positive regulation of inflammatory response (GO:0050729), were selected for illustration of underlying mechanisms. To investigate the inflammatory response regulated at the cellular level, we stained sections of hearts harvested on post-operative day 5 from ICR mice in the control, MI-only and cell sheet groups for the monocyte marker monocyte chemoattractant protein 1 (Mcp1) chemokine C–C motif ligand 2 (Ccl2), pro-inflammatory sub-type classical (M1) macrophage marker Cd68 and protective non-classical resident (M2) macrophage marker CX3C chemokine receptor 1 (Cx3cr1).

2.7. Heart tissue sections

On post-operative days 5 and 28, the mice were anesthetised with 3% isoflurane, sternotomy was performed to open the chest and perfusion was conducted using 2% heparin DPBS. The heart was cut off from the aorta and split from the ligation line.

For cryo-sectioning, tissue below the ligation line was placed in 4% paraformaldehyde for 8 h, then cryo-preserved using 20% sucrose for 4 h and 30% sucrose for 12 h and finally embedded in optimal-cutting-temperature compound; thereafter, 10-μm-thick sections were cut.

2.8. Detection of inflammation

For immunohistochemistry (IHC), the sections were immersed in 0.3% periodic acid to block intrinsic peroxidase, dissolved in 0.1% triton solution for 30 min and then treated with 10% donkey serum in 50 mM PBS for 1 h at room temperature to block any non-specific antibody response. After blocking, the sections were first incubated with primary antibodies overnight at 4 °C and then with the corresponding horseradish peroxidase-conjugated antibody for the diaminobenzidine reaction. The following primary antibodies were used: Mcp1, CD68 and Cx3cr1 (Detailed information of antibodies see Supplementary Table 1). The sections were observed under an Olympus BX-51 digital microscope camera (Olympus Optical Co., Japan) and analysed using Image-Pro Plus version 6.0 (Media Cybernetics, Rockville, MD, USA) by a double-blinded investigator. For each measurement in each mouse, we analysed 6 randomly selected 20 × regions per section (i.e. $n = 6$ measurements per mouse).

2.9. In vitro differentiation of THP-1 cells into macrophages and flow cytometric analysis of CD68 cytoplasmic expression

THP-1 (human myeloid leukaemia mononuclear cells) monocytes were cultured in RPMI1640 medium with 10% FBS and added to a six-well plate (2.5×10^5 cells/well) and induced to differentiate into M0 macrophages using 150 nM phorbol 12-myristate 13-acetate (PMA)

(Sigma-Aldrich, St. Louis, MO, USA) for 72 h. M0 macrophages were polarised similar to classical macrophages when treated with 20 ng/mL interferon gamma (IFN-γ) (PeproTech Inc, Rocky Hill, NJ, USA) and 10 pg/mL lipopolysaccharide (LPS) (Sigma-Aldrich), after co-culture with or without hUCMSCs in 0.4-μm Transwell chambers (Corning, NY, USA) for 48 h. Cells were washed twice with cold Dulbecco's phosphate-buffered saline [DPBS], centrifuged at 300×*g*, for 3 min at room temperature, and resuspended in 200 μL of Fixation/Permeabilisation solution (BD Biosciences, Bedford, MA, USA) for 10 min at room temperature. The cell suspension was centrifuged twice for 3 min at 600×*g* at room temperature, and the pellet resuspended each time with 1 ml of 1 × Perm/Wash buffer (BD Biosciences). Homogeneously resuspended cells in 100 μL were incubated with Fixation/Permeabilisation solution, 2 μL of an FITC anti-human CD68 Antibody (Biolegend, San Diego, CA, USA) or 2 μL of an isotype-specific FITC mouse IgG2bκ (Biolegend) and then incubated for 20 min at room temperature (Detailed information of antibodies see Supplementary Table 1). The suspension was centrifuged for 3 min at 600×*g* at room temperature and the pellet was washed once with 1 mL of 1 × Perm/Wash buffer. Cells were centrifuged at 600×*g* for 3 min, resuspended in 100 μL of DPBS and then analysed using a FACS CytoFLEX S (Beckman, Pasadena, CA, USA).

2.10. Quantification of angiogenesis

For immunofluorescence, the section were blocked with 10% donkey serum for 60 min at room temperature, incubated with primary antibodies overnight at 4 °C and re-incubated with the corresponding secondary antibodies (1:500, Alexa 555; Invitrogen) except Alexa Fluor™ 568-conjugated isolectin B4 (IB4) (Detailed information of antibodies see Supplementary Table 1). The sections were then mounted using Vectashield mounting medium containing DAPI (Vector Laboratories, Burlingame, CA, USA). The following antibodies were used: IB4 and α-smooth muscle actin (α-SMA). The sections were observed under a confocal laser microscope. IB4-positive neovessels and α-SMA-positive arterioles were counted using Zeiss Zen version 2.3 (Zeiss) by a double-blinded investigator. For each measurement in each mouse, we analysed 6 randomly selected regions per section (i.e. $n = 6$ measurements per mouse).

2.11. Echocardiography

On day 0 before surgery and days 7 and 28 post-MI, the mice were anesthetised with 1%–3% isoflurane until the heart rate stabilised at 400–550 bpm. Parasternal long-axis trace brightness-mode images and mitral inflow velocity were acquired using a high-resolution micro-ultrasound Vevo 2100 Imaging system (FUJIFILM VisualSonics Inc., Toronto, Ontario, Canada). To assess the heart diastolic function, the left ventricular (LV) ejection fraction (EF), fractional shortening (FS) and ratio of the early (*E*)/late (*A*) ventricular filling velocity using Vevo LAB analysis software (FUJIFILM VisualSonics Inc.) by a double-blinded operator. To accurately evaluate the heart strain function, we calculated the radial/longitudinal endocardial strain/strain rate, in addition to the strain peak percentage (Pk%) and strain rate peak per s (Pk 1/s) [48]. The radial/longitudinal endocardial strain/strain rate was analysed only in MI zones 5 and 6.

2.12. Masson staining and determination of fibrosis size and ventricular wall thickness

To evaluate the effect of the hUCMSC sheet on MI-induced cardiac fibrosis, we analysed sections of the heart sample harvested on day 28 post-MI. The MI size was calculated by staining sections of the LV-level papillary muscle along the short axis using Masson's trichome stain. In the hUCMSC sheet group, the transplanted sheet was removed before measurement. The MI zone fibrosis length (blue area) and LV wall thickness were measured using NPD View version 2.6.8 (Hamamatsu, Japan). The LV sections were divided into 12 areas per section, where areas 1–5 corresponded to the septal wall and areas 6–12 to the lateral wall. Segments 9–11 were labelled the MI zone, and segments 6–8 and 12 were labelled the border zone.

2.13. Statistical analysis

Data were analysed using SPSS Statistics version 26.0.0.1 (IBM Co., Armonk, NY, USA) and expressed as means ± standard deviation (SD). For all experiments, data were detected using one-way analysis of variance (ANOVA) with the Tukey comparison test, Welch ANOVA with the Games–Howell comparison test, Kruskal–Wallis *H* test with Bonferroni correction, two-way repeated-measures ANOVA with the least significant difference comparison (LSD) test or *t*-test. $P < 0.05$ was considered statistically significant. Data differences were represented as follows: ¯mean not appropriate for difference comparison; NS, no significance; *mean $P < 0.05$; **mean $P < 0.01$; and ***mean $P < 0.001$.

3. Results

3.1. Phenotypic characterisation of hUCMSCs and transplanted hUCMSC sheet

Flow cytometry-based characterisation detection of hUCMSCs isolated from donors showed that the cells were positive for CD73, CD90 and CD105 and negative for CD19, CD34, and CD45 (Supplementary Fig. 2). The Passages 4th hUCMSCs (Fig. 1A) for creating an hUCMSC sheet (Fig. 1B). DAPI staining showed a positive signal for fibronectin on the bottom (Fig. 1C) and a positive signal for β1-integrin on the entire hUCMSC sheet (Fig. 1D). These results indicated high adhesion ability.

After LAD ligation, the hUCMSC sheet transplanted on the surface of the heart, covering the MI zone, during the surgical process of generating an AMI mouse model (Fig. 1E). Post-operatively, the mice showed typical AMI features, such as ST segment elevation on electrocardiography (Fig. 1F).

3.2. Cell sheet form enhances hUCMSC survival and retention

The bio-luminescent imaging (BLI) intensity signal of luciferase-hUCMSCs generated via the luciferase-expressing lentivirus (Supplementary Fig. 3) was positively linear and correlated with the hUCMSC number (Fig. 2A).

In ICR mice, on post-operative days 1, 3, 5, 7, 9 and 11, the BLI signal was significantly stronger in the cell sheet group compared with the suspension group. A weak BLI signal was detected on days 30 and 60 in the cell sheet used to treat NOD/SCID mice (Fig. 2B). The hUCMSC retention time was <5 days in the suspension group (purple line), >9 days in the ICR mice in the cell sheet group (blue line) and >60 days in NOD/SCID mice in the cell sheet group (Fig. 2C, orange line);

The hearts of ICR mice in the cell sheet group transplanted with the hUCMSC sheet on days 1, 5, 9, and 28 (Fig. 2D). As observed in the histological image of the hUCMSC sheet-coated area, the hUCMSC sheet was viable and formed a solid connection with the host epicardium (Fig. 2E). On post-transplantation day 1, we found a significant portion of HNA-negative nonhuman cells inside the hUCMSC sheet (Fig. 2F), indicating that the host inflammatory cells were remarkably infiltrated. On post-transplantation day 5, the host inflammatory cells disappeared and the human cells in the hUCMSC sheet decreased. On post-transplantation day 9, fewer human cells survived and more nonhuman host cells were grafted in the sheet tissue. On post-transplantation day 28, no human cells remained, and the cells were completely replaced by host cells in the sheet area (Fig. 2F).

Collectively, these findings showed that the sheet form significantly enhances hUCMSC retention and survival. Further, most hUCMSCs did not survive beyond day 11 in ICR mice, although slightly longer in NOD/

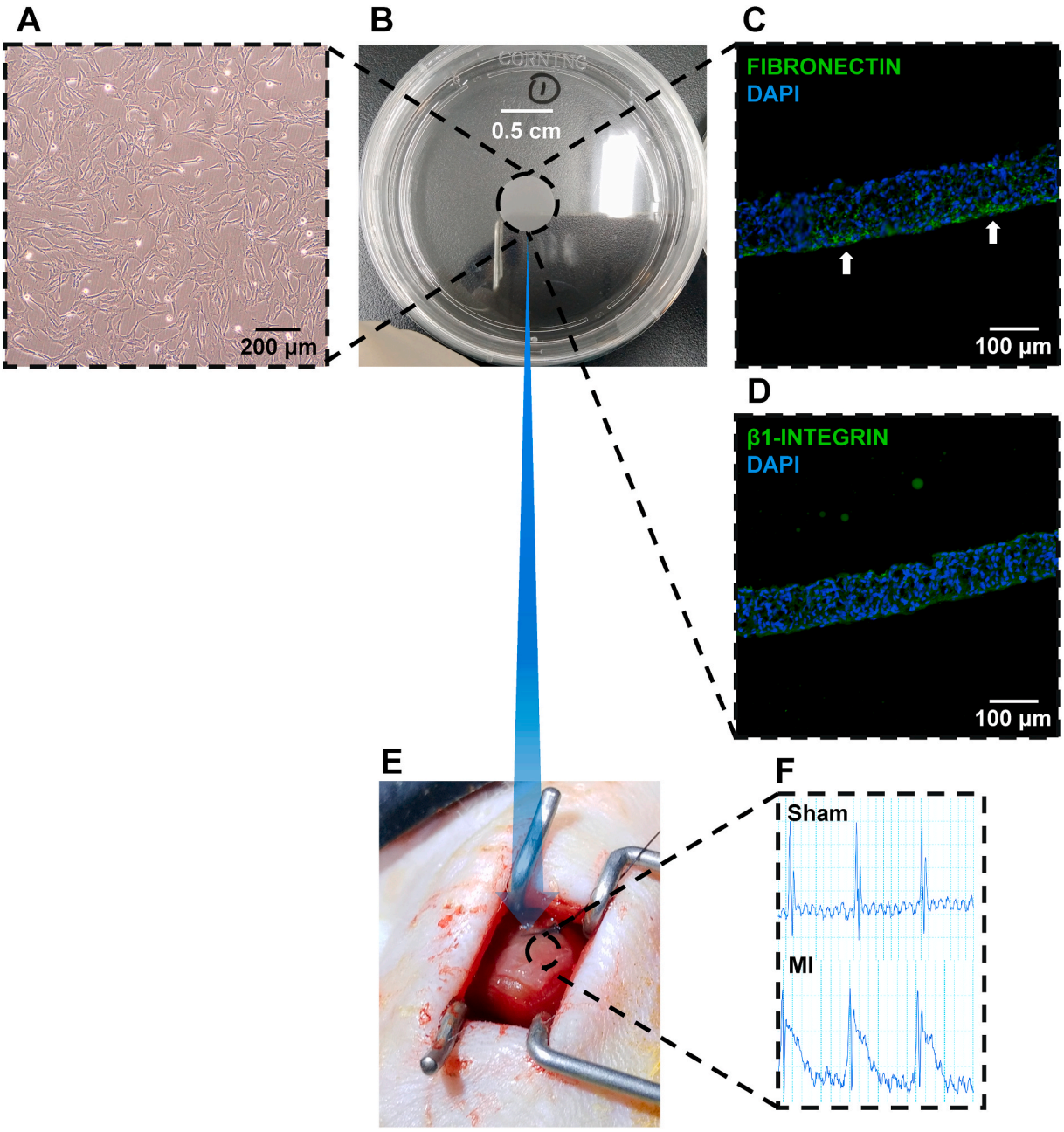

Fig. 1. Phenotypic characterization of the hUCMSC sheet and transplantation in an AMI mouse model. (A) hUCMSCs isolated from the donor umbilical cord at P4 cell morphology stage. Scale bar = 200 μm. (B) hUCMSCs cultured in a temperature-responsive culture dish overnight; sheet formation can be seen. (C) Immunostaining of hUCMSC sheet demonstrated the expression profile of fibronectin (green). Cells were also counterstained with DAPI for nuclei (blue). Scale bar = 100 μm. (D) Immunostaining of hUCMSC sheet demonstrated the expression profile of β1-integrin (green). Cells were also counterstained with DAPI for nuclei (blue). Scale bar = 100 μm. (E) AMI mouse model established and hUCMSC sheet transplanted to cover the ischemic location. (F) Electrocardiogram monitoring indicating the MI group showed ST segment elevation. hUCMSC, human umbilicalcord mesenchymal stem cell; AMI, acute myocardial infarction; DAPI, 4′,6-diamidino-2-phenylindole; MI, myocardial infarction. (For interpretation of the references to colour in this figure legend, the reader is referred to the Web version of this article.)

SCID mice, suggesting that after hUCMSCs transplantation, immunological rejection occurred within 11 days, and hUCMSC sheet intervention for MI is highly possible within 11 days after transplantation.

3.3. hUCMSC sheet alleviates post-MI inflammation by monocyte and macrophage regulation for myocardium protection

The inflammatory cascade plays a critical role in response to ischaemic heart injury, with inflammation having a double-sided effect. To test whether hUCMSC sheet can mitigate post-MI myocardial inflammation, we analysed the transcriptional profiles of myocardial tissue collected 5 days post-MI ischaemic injury and found 173 DEGs (Supplementary Fig. 4, Supplementary Table 2).

Proinflammatory chemokines, such as monocyte chemoattractant protein-1 (Mcp1) and chemokine C–C motif ligand 2 (Ccl2), played an important role in inflammatory cascades in an infarcted heart [49]. Cd68-positive classical macrophages are a proinflammatory subtype that overexpresses inflammatory genes [50], whereas Cx3cr1-positive nonclassical polarised macrophages are essential for MI repair [51].

The expression level of the inflammatory response-related gene *Ccl2* in the MI-only group was higher and that of the inflammatory repressive gene *Cx3cr1* was lower in the MI-only group compared with the cell

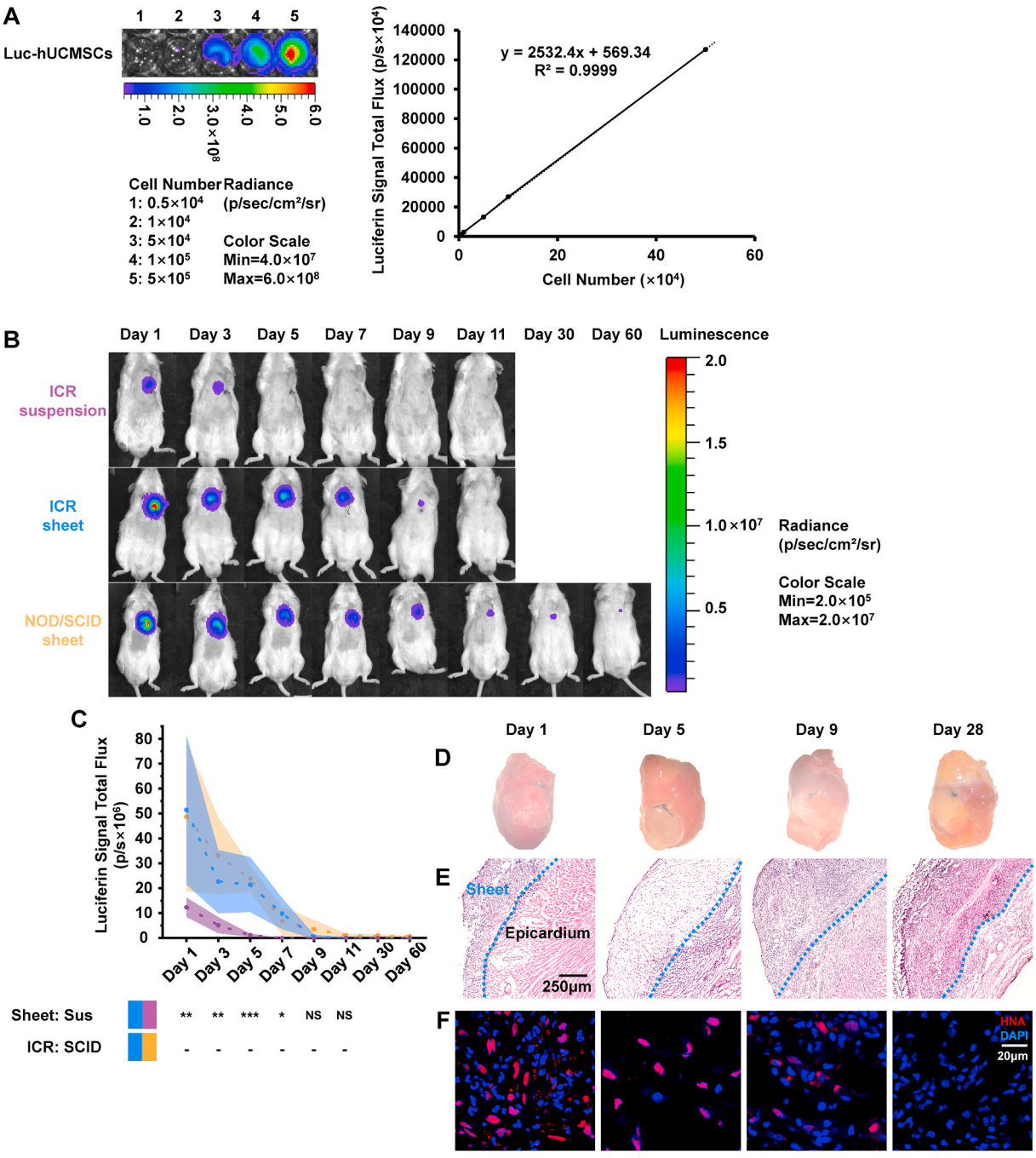

Fig. 2. Retention and survival of implanted hUCMSC sheet and hUCMSC suspension in an AMI mouse model. (A)Known quantities of expressing luciferase-hUCMSCs were measured and utilized to establish a standard curve creating a relationship between cell number and luciferin signal intensity. (B) MI-induced ICR or NOD/SCIDmice were implanted with luciferase-hUCMSC suspension or sheet, which constitutively expressed luciferase. Post-MI and after luciferase-hUCMSC transplantation day 1, BLI was done every other day until day 11; BLI ofNOD/SCID mice with the luciferase-hUCMSC sheet was done at days 30 and 60. (C) Luciferin signal intensity compared among hUCMSC suspension with ICR mice (n = 9), hUCMSC sheet with ICR mice (n = 9) andhUCMSC sheet with NOD/SCID mice (n = 4). The values were mean (solid line) ±SD (shadow). (D) Post hUCMSC sheet transplantation in ICR mice; the hUCMSC sheet-connected heart morphological characterization. (E)Inter-tissue connection between hUCMSC sheet and the epicardium. (F) Immunostaining of hUCMSC sheet with anti-HNA (red) and counter-stained with DAPI for nuclei (blue).Scale bar = 20 μm **Cell sheet group (blue) >suspension group (purple) with ICR mice on days 1 and 3 post-operatively ($P < 0.01$); ***Cell sheet group (blue) > suspension group (purple) with ICR mice on day 5 post-operatively ($P < 0.001$); *Cell sheet group >suspension group with ICR mice on day 7 post-operatively ($P < 0.05$), by two-way ANOVA with LSD comparison test (C). hUCMSC, human umbilical cord mesenchymal stem cell; AMI, acute myocardial infarction; MI,myocardial infarction; ICR, Institute of Cancer Research; NOD/SCID, non-obese diabetic/severe combined immune deficiency; BLI, bio-luminescent imaging; SD, standard deviation; Sus, suspension; HNA, human nucleiantigen; DAPI, 4′,6-diamidino-2-phenylindole; ANOVA, analysis of variance; LSD, least significant difference. (For interpretation of the references to colour in this figure legend, the reader is referred to the Web version of this article.)

sheet group (Fig. 3A). We used IHC staining detected the cell sheet, cell suspension and MI-only groups with monocyte marker Mcp1. Results showed that the cell sheet group had significantly fewer Mcp1-positive monocytes compared with the MI-only group, although there was no significant difference between the MI-only and cell suspension groups (Fig. 3E). The cell sheet group had significantly fewer CD68-positive macrophages compared with the cell-suspension and MI-only groups (Fig. 3F). In addition, the number of Cx3cr1-positive non-classical macrophages increased in the cell sheet group compared with the cell suspension and MI-only groups (Fig. 3G). The *in vitro* experiment demonstrated that the co-cultured hUCMSCs significantly reduced the M0 macrophage-derived CD68-positive classical macrophages rate (Supplementary Fig. 5, Fig. 3H).

These findings suggest that the transplanted hUCMSC sheet

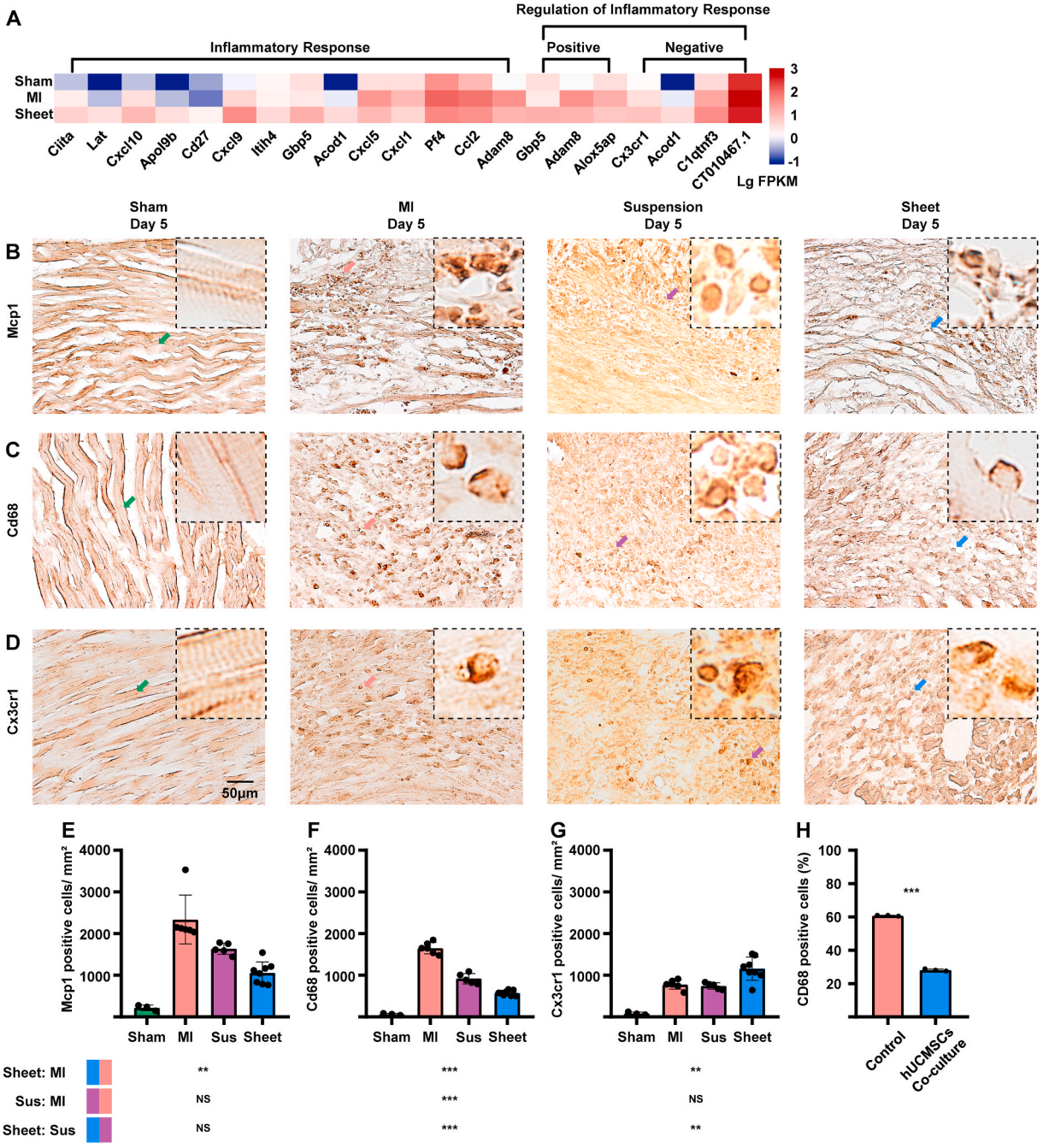

Fig. 3. Evaluation of inflammatory effects in the ischemic heart injury area of ICR mice. (A)Transcriptome array and GO:BP analysis with inflammatory response-related genes (n = 2, each group). (B) IHC staining of treatment and MI-only groups 5 days post-MI with monocyte marker Mcp1. Scale bar = 50 μm (C)IHC staining of treatment and MI-only groups 5 days post-MI for the M1 macrophage marker Cd68. Scale bar = 50 μm. (D) IHC staining of treatment and MI-only groups 5 days post-MI with non-classical macrophagemarker Cx3cr1. Scale bar = 50 μm. (E–G) Quantitative analysis of Mcp1-, Cd68-and Cx3cr1-positive cells/mm2; values are mean ± SD (control group, n = 3; MI-only group, n = 6; suspension groups, n = 5; cell sheet group,n = 8). NSCell sheet group (blue) < cell suspension group (purple) with Mcp1-positive cells (P > 0.05); Kruskal–Wallis H test with Bonferroni correction (E); ***cell sheet group (blue) < cell suspension group (purple) withCD68-positive cells (P < 0.001); **cell sheet group (blue) < cell suspension group (purple) with Cx3cr1-positive cells (P < 0.01) by one-way ANOVA with Tukey comparison test (F, G), ***hUCMSCs co-cultured group >control group with CD68-positive cells rate (P < 0.001); *t*-test. GO:BP, Gene Ontology Biological Process; IHC, immunohistochemistry; MI, myocardial infarction; Sus, suspension; Mcp1, monocyte chemoattractant protein 1; SD, standard deviation; ANOVA, analysis of variance. (For interpretation of the references to colour in this figure legend, the reader is referred to the Web version of this article.)

modulates inflammation in the infarcted myocardium presumably by down-regulating pro-inflammatory macrophages and up-regulating protective macrophages. Cell sheet transplantation has greater potential to modulate inflammation in the MI myocardium compared with the hUCMSC suspension.

3.4. hUCMSC sheet promotes angiogenesis in the MI border zone

hUCMSC sheet treatment augmented the preservation or formation of the neovessel response by immunostaining for IB4 (Fig. 4A) and the arteriole response by immunostaining for α-SMA (Fig. 4B). The

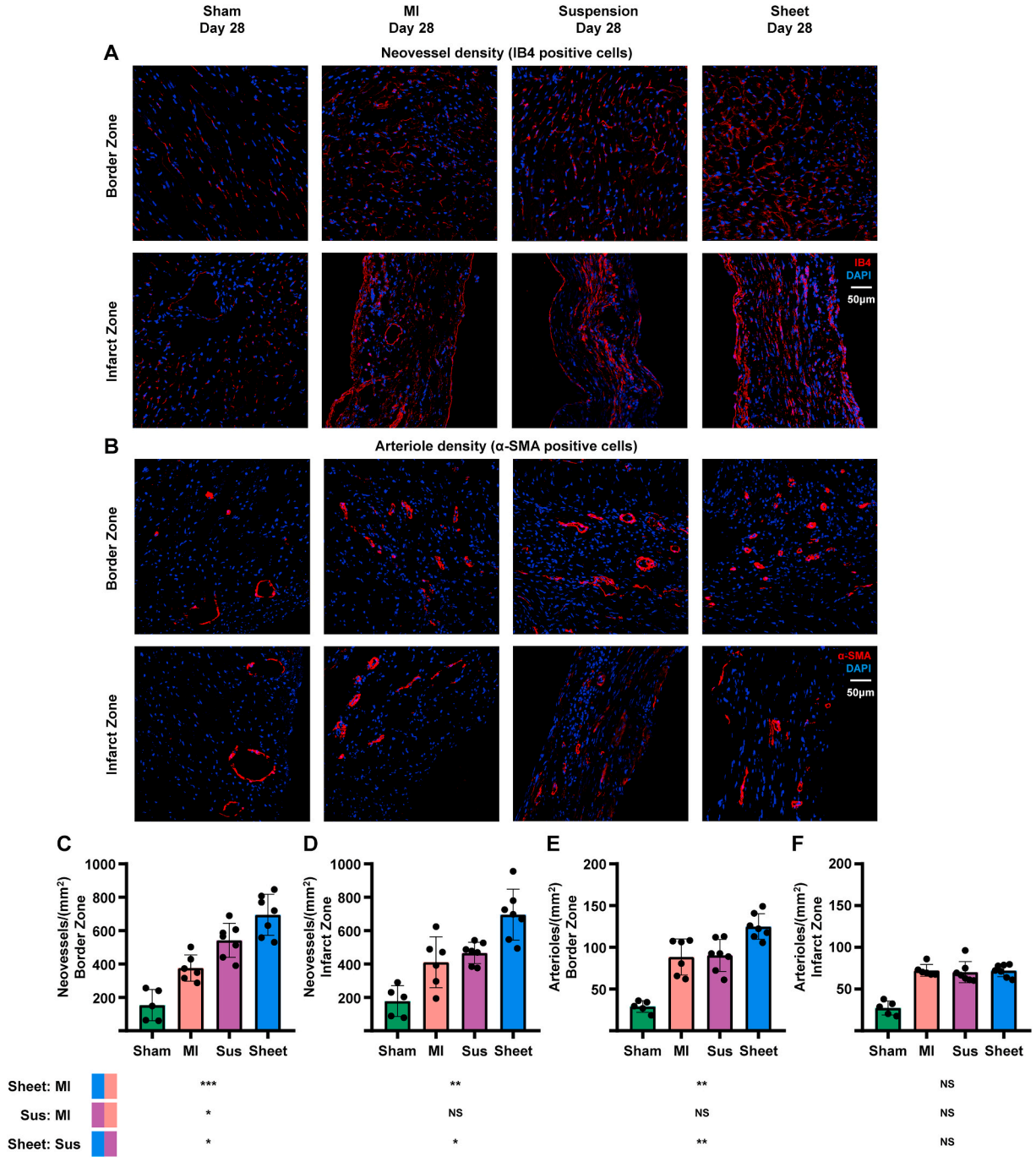

Fig. 4. Assessment of angiogenesis post-MI of ICR mice. (A)Immunostaining of treatment and MI-only groups at day 28 post-MI with neovesselmarker IB4 (red) and counterstained with DAPI for nuclei (blue) in ischemic heart injury border zone and infarct zone, respectively.Scale bar = 50 μm. (B) Immunostaining of treatment and MI-only groups at day 28 post-MI with smooth muscle marker (α-SMA) (red) and counterstained with DAPI for nuclei (blue) in ischemic heart injury border zone andinfarct zone, respectively. Scale bar = 50 μm. (C–F) Quantitative analysis of IB4-and α-SMA-positive cells/mm2; values are means ± SD (control group, n = 5; MI-only group, n = 6; suspension groups, n = 7; cell sheetgroup, n = 7). *Cell sheet group (blue) > cell suspension group (purple) with IB4-positive neovessels in border zone ($P < 0.05$); *cell sheet group (blue) > cell suspension group (purple) with IB4-positive neovessels in infarctzone ($P < 0.05$); NScell sheet group (blue) > cell suspension group (purple) with α-SMA-positive arterioles in infarct zone ($P > 0.05$); one-way ANOVA with Tukey comparison test (C, D, F); **cell sheet group (blue) > cellsuspension group (purple) with α-SMA-positive arterioles in border zone ($P < 0.01$); Kruskal–Wallis H test with Bonferroni correction (E); . MI, myocardial infarction; Sus, suspension; IB4, isolectin B4; DAPI, 4′,6-diamidino-2-phenylindole; α-SMA, α-smooth muscle actin; SD, standard deviation; ANOVA, analysis of variance. (For interpretation of the references to colour in this figure legend, the reader is referred to the Web version of this article.)

neovessel density in the cell sheet group was significantly higher compared with cell suspension and MI-only groups in the border and infarct zones (Fig. 4C and D). In addition, arteriole formation was significantly higher in the cell sheet group compared with the cell suspension and MI-only groups in the border zone but not in the infarct zone (Fig. 4E and F).

These findings show that the hUCMSC sheet had greater potential to promote angiogenesis in the ischaemic heart compared with the hUCMSC suspension.

3.5. hUCMSC sheet improves cardiac function

Echocardiographic assessments of LV long-axis functions, such as EF and FS via end systolic or diastolic volume (Fig. 5A), were comparable among the sham control (Fig. 5B and C, green), MI-only (Fig. 5B and C, red), cell suspension (Fig. 5B and C, purple) and cell sheet (Fig. 5B and C, blue) groups before MI (Day 0). The EF values were significantly higher in the cell sheet group than those in the cell suspension and MI-only groups (Fig. 5B and C) at days 7 and 28 post-MI. The FS were significantly higher in the cell sheet group compared with both cell suspension and MI groups (Fig. 5B and C) at day 28 post-MI. In addition, in the cell sheet group, we found no significant changes in the EF and FS between days 7 and 28 post-MI; however, the EF and FS progressively decreased between days 7 and 28 post-MI in the cell suspension and MI-only groups, whereas they were not significantly different between days 7 and 28 post-MI in the cell sheet group (Fig. 5B and C). Supplementary Fig. 6 shows the left ventricular end systolic and end diastolic volumes. The mitral *E* and *A* peak values observed at day 28 post-MI (Fig. 5D) were significantly higher in the cell sheet group (Fig. 5E, blue) compared with the cell suspension (Fig. 5E, purple) and MI-only (Fig. 5E, red) groups. Supplementary Fig. 7 shows the endocardial radial/longitudinal strain and strain rate in the injury area, and Fig. 5F–I shows the strain peak percentage (Pk%) and strain rate peak per second (Pk 1/s). The radial strain, the longitudinal strain and the longitudinal strain rate were significantly higher in the cell sheet group compared with those in the MI-only group (Fig. 5F, G, I), whereas the radial/longitudinal strain and strain rate were not significantly different between the MI-only and cell suspension groups (Fig. 5F–I).

These findings demonstrated that the hUCMSC sheet had greater potential to prevent ischaemia-induced loss of cardiac function compared with the hUCMSC suspension.

3.6. hUCMSC sheet decreases cardiac fibrosis

We investigated the morphological characterisation and Masson staining of heart samples harvested on post-MI day 28 (after cell sheet removal) (Fig. 6A). We illustrated the overall cardiac fibrosis via a clock segment graph (Fig. 6B). Cardiac fibrosis significantly decreased in the cell sheet group compared with the MI-only group; however, there was no significant difference between the MI-only and cell suspension groups (Fig. 6C).

There was no significant difference in LV wall thickness in the infarct zone among cell sheet, cell suspension, and MI-only groups (Fig. 6D). In the border zone, LV wall thickness was significantly higher in the cell sheet group compared with cell suspension and MI-only groups (Fig. 6E). In the remote zone, LV wall thickness was significantly higher in the cell suspension and MI-only groups compared with cell sheet group (Fig. 6F).

These findings suggested that the hUCMSC sheet has greater potential to prevent cardiac fibrosis in the ischaemic border zone but not in the MI zone compared with the hUCMSC suspension.

4. Discussion

The present study is the first to report the safety and efficacy of hUCMSC sheets in an AMI mouse model. Regarding the principal and novel findings of the present study, the applied cell sheet technology (Fig. 1) significantly improved the retention rate of hUCMSCs (Fig. 2), regulated the inflammatory response (Fig. 3) and promoted angiogenesis in the MI border (Fig. 4), improved cardiac function (Fig. 5), and reduced harmful ventricular remodelling (Fig. 6). Moreover, we determined the efficient intervention time of hUCMSC sheets in the present AMI model mice for the first time (Fig. 2).

Stem cell-based therapy is a promising way of treating ischaemic heart disease. The hUCMSC sheet method used in the present study improves hUCMSC retention and survival post-transplantation into MI mice, leading to a better therapeutic effect. Interestingly, most cells inside the hUCMSC sheet can only survive in the epicardium for ~1 week in ICR mice, and only a few cells remain alive for >8 weeks in SCID mice without any immunorejection. Therefore, in this study, we could target the main intervention time of the hUCMSC sheet for MI within 1 week post-transplantation. In the future clinical application of allogenic hUCMSC transplantation, it would be difficult to completely inhibit patient immunorejection. Therefore, outcomes from ICR mice could better evaluate the benefits on cardiac function and the underlying mechanisms.

At the initial stage of AMI (day 0–3), the host heart was immersed in considerably numerous inflammatory cells that infiltrated the cell sheet. Thus, anti-inflammation is the main therapeutic effect of hUCMSC sheet, probably via paracrine secretion and direct cell–cell contact. After the acute inflammation (day 4–11), the hUCMSCs that survived kept producing the extracellular matrix and provided mechanical support to the host heart. After post-transplantation day 12, the hUCMSCs died out and the remaining extracellular matrix served as an excellent bioactive scaffold. Then, the host cells gradually migrated into the scaffold, eventually form a piece of living epicardial tissue. During this process, the bioactive scaffold not only built its vascular structure but also facilitated the angiogenesis of the host peri-infarction area by providing new routes for the vascular cells (Fig. 7).

One of the advantages of using scaffold-free cell sheet technique for *in vivo* studies of MI is that the transplanted cells can be recovered and made to undergo unbiased testing, such as multi-omics analysis. In future research, this technique will be further assessed to determine the kind of environment the cell sheet provides in the epicardium and clarify the overall mechanism of action.

Heart failure is one of the most serious complications of MI and is closely related to changes in cells, molecules and proteins in myocardial tissue post-MI. The inflammatory response caused by cell necrosis post-MI can mobilise various immune cells in the body to participate in the elimination of necrotic substances. The inflammatory cascade plays a critical role in the response to ischaemic heart injury. In addition, selective activation of chemokine-dependent recruited cells can promote angiogenesis in the injury area. However, an excessive inflammatory response can cause additional damage to the tissues surrounding the MI area and lead to poor ventricular remodelling and impaired myocardial function. Therefore, effective regulation of the inflammatory response in the early stage of MI is the core factor that determines whether severe heart failure will occur. Accordingly, we investigated the regulation of inflammation caused by hUCMSC sheet as well as tested the effects of inflammation involved in the angiogenesis promotion, heart function preservation and ventricular remodelling inhibition.

Prolonged coronary artery occlusion causes cell death, triggering a strong inflammatory response. A recent study reported that cell therapy repairs ischaemic heart injury through an acute sterile immune response by Cx3cr1-positive macrophages [51]. The classic macrophage marker Cd68 causes inflammation damage after ischaemic heart injury. The hUCMSC sheet can decrease Mcp1-positive monocytes and classical CD68-positive macrophages in the early stage (5 days post-MI) of ischaemic myocardial injury, indicating that the hUCMSC sheet can effectively decrease inflammation-induced cardiac injury and prevent cardiac damage. Increased activation of Cx3cr1-positive cells at the injured myocardium also implicates the protective inflammatory

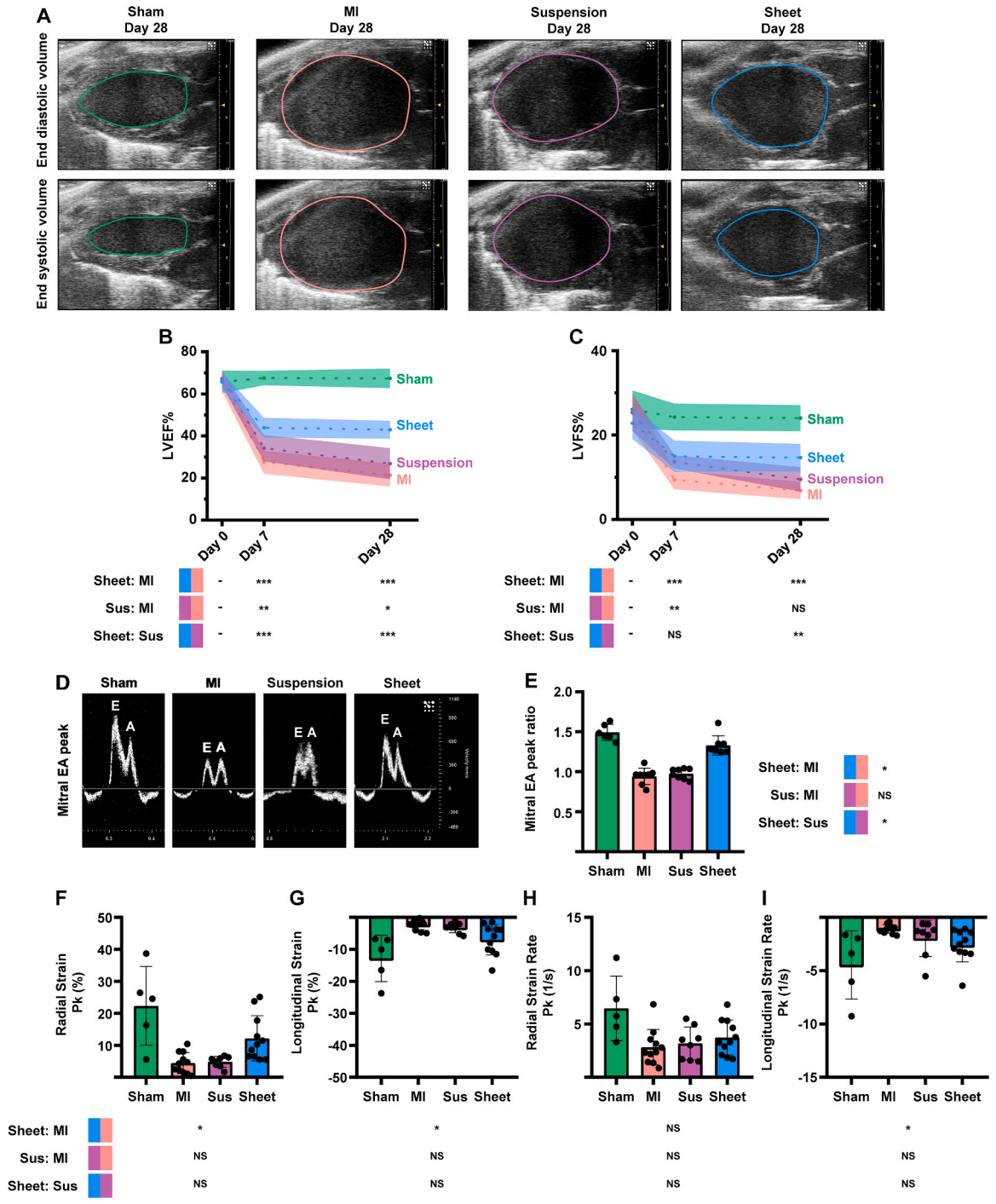

Fig. 5. Transplantation of hUCMSC sheet preserves cardiac function of ICR mice. (A)Echocardiograph LV long-axis end diastolic/systolic volume images of treatment and MI-only groups at day 28 post-MI. (B, C) Assessment of echocardiograph LV long-axis EF and FS before MI in treatment and MI-only groups at days 7 and 28 post-MI (control group, n = 6; MI-only group, n = 16; suspension groups, n = 8; cell sheet group, n = 16); values are means (solid line) ±SD (shadow). (D) Peak of the mitral early (E)/late (A)ventricular filling velocity images in treatment and MI-only groups at day 28 post-MI. (E) Quantitative analysis of mitral E/A peak ratio; values are means ± SD (control group, n = 6; MI-only group, n = 8; suspension groups,n = 8; cell sheet group, n = 8). (F–I) Quantitative analysis of radial/longitudinal strain and strain rate; values are means ± SD (control group, n = 5; MI-only group, n = 11; suspension groups, n = 8; cell sheet group, n = 11).*** and NScell sheet group (blue) > cell suspension group (purple) with EF and FS at day 7 post-operatively ($P < 0.001$ and $P > 0.05$); *** and **Cell sheet group (blue) > cell suspension group (purple) with EF and FS atday 28 post-operatively ($P < 0.001$ and $P < 0.001$); **cell sheet group (blue) > cell suspension group (purple) with FS at day 28 post-operatively ($P < 0.01$); NScell sheet group (blue) with EF and FS at days 7 and 28 post-operatively ($P > 0.05$); ** and *cell suspension group (purple) with EF and FS at days 7 and 28 post-operatively ($P < 0.01$ and $P < 0.05$); two-way ANOVA with LSD comparison test (B, C); *cell sheet group (blue) > cellsuspension group (purple) with mitral E/A peak ratio ($P < 0.05$); Kruskal–Wallis H test with Bonferroni correction (E); *cell sheet group (blue) > MI-only group (red) with radial strain ($P < 0.05$); *cell sheet group (blue) < MI-only group (red) with longitudinal strain rate ($P < 0.05$); Kruskal–Wallis H test with Bonferroni correction (F, I); *cell sheet group (blue) < MI-only group (red) with longitudinal strain ($P < 0.05$); Welch ANOVA with Games–Howell comparison test (G); NScell sheet group (blue) > MI-only group (red) with radial strain rate ($P > 0.05$); one-way ANOVA with Tukey comparison test (H). hUCMSC, human umbilical cord mesenchymal stem cell; LV, left ventricular; MI, myocardial infarction; Sus, suspension; EF, ejection fraction; FS, fractional shortening; SD, standard deviation; ANOVA, analysis of variance; LSD, least significant difference. (For interpretation of the references to colour in this figure legend, the reader is referred to the Web version of this article.)

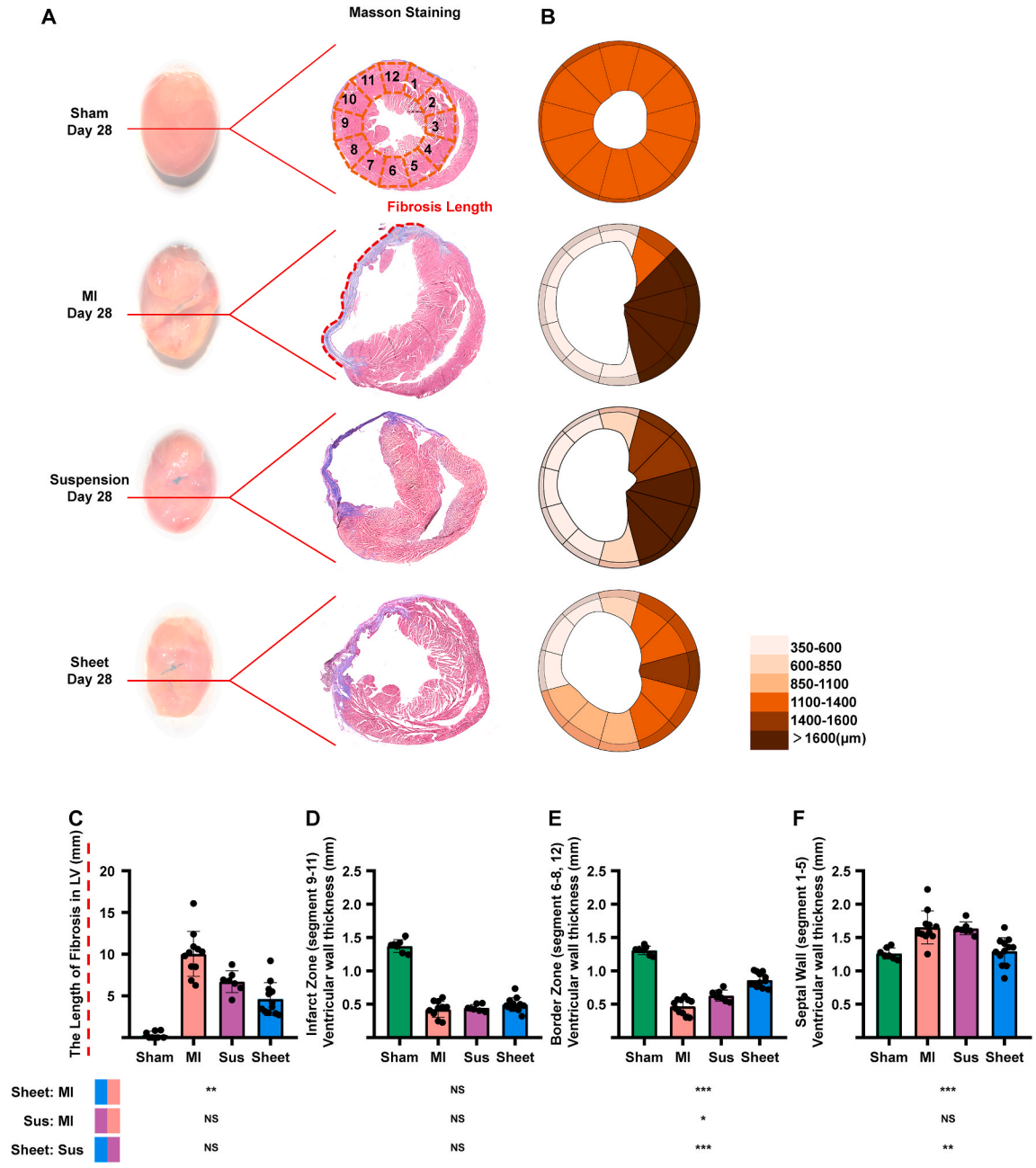

Fig. 6. hUCMSC sheet treatment decreased cardiac fibrosis in ischemic heart injury border zone post-MI of ICR mice. (A)Heart morphological characterization and Masson staining of treatment and MI-only groups at day 28 post-MI: fibrosis area (blue) and myocytes (red). (B) Quantitative analysis of LV wall thickness in 12 segmentsindividually; values are mean ± SD (control group, n = 7; MI-only group, n = 11; suspension groups, n = 7; cell sheet group, n = 12). (C) Quantitative analysisof infarct zone fibrosis length; values are mean ± SD (controlgroup, n = 7; MI-only group, n = 11; suspension groups, n = 7; cell sheet group, n = 12). (D–F) Quantitative analysis of LV wallthickness in border zone, infarct zone and septal wall, respectively; values are mean ± SD(control group, n = 7; MI-only group, n = 11; suspension groups, n = 7; cell sheet group, n = 12). NScell sheet group (blue) > cell suspension group (purple) with infarct zone fibrosis length ($P > 0.05$); Kruskal–Wallis H test with Bonferroni correction (C); NScell sheet group (blue) > cell suspension group (purple) with LV wall thickness in infarct zone ($P > 0.05$); ***cell sheet group (blue) > cell suspension group (purple) with LV wall thickness inborder zone ($P < 0.001$); **cell sheet group (blue) < cell suspension group (purple) with LV wall thickness in septal wall ($P < 0.01$); one-way ANOVA with Tukey comparison test (D–F). hUCMSC, human umbilical cordmesenchymal stem cell; MI, myocardial infarction; Sus, suspension; LV, left ventricular; SD, standard deviation; ANOVA, analysisof variance. (For interpretation of the references to colour in this figure legend, the reader is referred to the Web version of this article.)

modulation of the hUCMSC sheet. However, since Cx3cr1-positive cells can be derived from resident monocytes or recruited from other organs via circulation, further investigation is required for elucidating the mechanism of activating Cx3cr1-positive cells.

Overall, our present data, for the first time, demonstrated that the hUCMSC sheet can regulate the inflammatory response in AMI model mice by both protective inflammatory modulation and deleterious inflammatory reaction, leading to cardiac function improvement. Hence, the comprehensive effect of inflammatory regulation from two directions could play a pivotal role on stem cell sheet intervention in AMI. Therefore, combining stem cell sheet intervention and inflammatory regulation therapy could more dramatically improve cardiac function and attain a better therapeutic outcome in AMI. However, it has to be clarified because adverse side effects and the necessity of

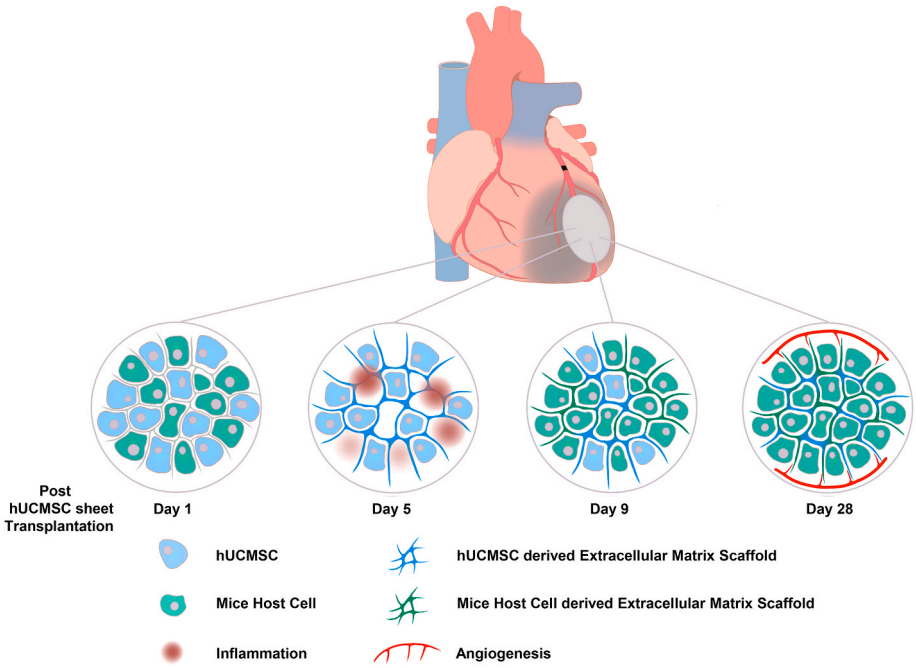

Fig. 7. Mechanisms of hUCMSC sheet mediated myocardial infarction therapy.

protective inflammatory response, traditional anti-inflammatory drugs, such as glucocorticoids, cannot be administered to MI patients [52]. Therefore, in-depth research is required to elucidate the mechanism underlying hUCMSC sheet-mediated biological immunomodulation. Particularly, the inflammatory reaction changes in different AMI phases, more specific effects and the origin of various inflammatory factors should be accurately elucidated in follow-up studies.

However, a fundamental question is whether hUCMSC sheet treatment can improve cardiac function. The LV long-axis trace method of evaluating the EF and FS can decrease human error due to selection of the short axis cross-section, increasing the accuracy of results. The major protective effects of the hUCMSC sheet occur within 7 days post-MI and post-transplantation. This time frame is also the critical period for regulation of the inflammatory response. No significant decrease in the EF and FS because of hUCMSC sheet treatment might be related to better preservation of cardiac tissue and enhanced angiogenesis. The diastolic function of the heart is one of the important indicators of ventricular remodelling with poor response. The *E/A* peak ratio, as a representative result of the diastolic function of the heart, is an important indicator for assessing adverse remodelling. The hUCMSC-enhanced long-term diastolic function might be because of previous inflammation regulation and angiogenesis. Speckle-tracking imaging is a sensitive technique for assessing myocardial tissue function. Strain can indicate the myocardial deform capability, and strain rate indicates the deformation speed. Stem cell-based MI treatment could increase the survival of cardiomyocytes and prevent further adverse ventricular remodelling [26,53,54]. The effect of the hUCMSC sheet group on intervention of MI was indicated by the longitudinal strain rate and radial/longitudinal strain, but not by the radial strain rate. We believe it is reasonable to conclude that this is explained by the greater amplitude of movement in the direction of the long axis, which was statistically significant. Our demonstration here that the hUCMSC sheet decreases fibrosis in the ischaemic border zone, but with limited effect in the MI zone, is consistent with the findings for arterial angiogenesis.

Transplantation of various stem cell sheets to treat heart failure after MI is one of the areas of focus for current research [22]. For example, some studies focused on how to improve the retention efficiency of stem cell sheets [55], whereas others focused on angiogenesis mechanism to intervene in an infarcted myocardium [56]. In our study, even if the hUCMSCs in the hUCMSC sheet gradually disappeared 9 days after transplantation, it can benefit from the heart function of mice. Therefore, the intervention time of hUCMSC sheet is mainly concentrated within 1 week after transplantation. Through our unbiased RNA sequencing, we found that inflammatory regulation is the main research direction. To our knowledge, this study is the first to conduct an *in vivo* study focusing on hUCMSC sheet intervention in MI.

We therefore believe that the hUCMSC sheet interfered with angiogenesis and fibrosis of the MI border zone by regulating the inflammatory response during the early stage of MI, which is reflected by heart function.

5. Conclusion

hUCMSCs sheet treatment can dramatically improve cardiac function post-MI in a mouse model. The biological function of hUCMSCs can be significantly enhanced in the form of a cell sheet, which provides superior local hUCMSC retention and survival. By modulating the inflammatory response in the MI border zone, the hUCMSC sheet improved cardiac function, eventually alleviating pathogenic remodelling. In addition, the hUCMSC sheet can be produced from standardised cryo-preserved cell stocks within 2–3 days in a scalable manner. However, these results are limited by the mouse model used; therefore, hUCMSC sheet should be tested in large animal MI models that are more clinically relevant. Nevertheless, the hUCMSC sheet is a promising treatment for ischaemic heart disease.

Declaration of competing interest

The authors have declared that no competing interest exists.

Acknowledgements

We thank Li Chen, Dr. Yu Zhao, Dr. Lei Tian and Dan Liu for assistance with IHC and THP-1 cell culture experiments. BOE Regenerative Medicine Technology Co. performed the preparation and identification of the hUCMSC sheets.

Abbreviations

hUCMSC	human umbilical cord mesenchymal stem cell
MI	myocardial infarction
PSCs-CMs	pluripotent stem cell-derived cardiomyocytes
hESCs	human embryonic stem cells
hMSCs	human mesenchymal stem cells
AMI	acute myocardial infarction
SPF	specific-pathogen-free
GMP	good manufacturing practices
MEM	minimum Essential Medium
FBS	foetal bovine serum
P4	fourth passage
P5	fifth passage
DAPI	4′,6-diamidino-2-phenylindole
ICR	institute of Cancer Research
NOD/SCID	non-obese diabetic/severe combined immune deficiency spontaneous mutation
LAD	left anterior descending
WT	wild-type
cDNA	complementary DNA
PCR	polymerase chain reaction
mRNA	messenger RNA
GO:BP	gene Ontology Biological Process
FPKM	fragments per kilobase per million mapped fragments
DEGs	differentially expressed genes
Mcp1	monocyte chemoattractant protein 1
C–C motif	chemokine
Ccl2	ligand 2
Cx3cr1	CX3C chemokine receptor 1
RPMI	Roswell Park Memorial Institute
PMA	phorbol 12-myristate 13-acetate
IFN-γ	interferon gamma
LPS	lipopolysaccharide
IHC	immunohistochemistry
IB4	isolectin B4
α-SMA	α-smooth muscle actin
LV	left ventricular
EF	ejection fraction
FS	fractional shortening
E/A	early/late
SD	standard deviation
BLI	bio-luminescent imaging
HNA	human nuclei antigen

Appendix A. Supplementary data

Supplementary data to this article can be found online at https://doi.org/10.1016/j.bioactmat.2021.01.036.

Funding

This work was supported by the Peking University Third Hospital Key Clinical Foundation [grant numbers BYSY2015007, BYSY2018039 and BYSYDL2019016 to Y.L.]; the capital health research and development of special [grant number 2020-2-4096 to Y.L.]; the Beijing Natural Science Foundation [grant number Z190013 to F.L.]; and the National Natural Science Foundation of China [grant number 81970205 to F.L.].

Author contribution statement

Rui Guo, Yunpeng Ling and Feng Lan designed the concept. Rui Guo wrote the manuscript, designed figures and tables. Shuang Gao and Dehua Chang performed hUCMSC sheet preparation and identification. Rui Guo, Hang Yang and Yichen Gong performed animal operations. Rui Guo and Tian Feng performed heart tissue staining, and double-blinded analysis. Rui Guo and Qing Xu performed echocardiography, and double-blinded analysis. Rui Guo and Shuhong Ma performed Bio-Luminescent Imaging, and double-blinded analysis. Masatoshi Morimatsu, Yunpeng Ling, Feng Wan, Heqing Wang and Feng Lan revised the manuscript. Hongjia Zhang provided an animal experiment platform. Yun Chang, Siyao Zhang and Youxu Jiang provided Animal Care.

References

[1] G.S. Abela, J.K. Kalavakunta, A. Janoudi, D. Leffler, G. Dhar, N. Salehi, J. Cohn, I. Shah, M. Karve, V.P.K. Kotaru, V. Gupta, S. David, K.K. Narisetty, M. Rich, A. Vanderberg, D.R. Pathak, F.E. Shamoun, Frequency of cholesterol crystals in culprit coronary artery aspirate during acute myocardial infarction and their relation to inflammation and myocardial injury, Am. J. Cardiol. 120 (10) (2017) 1699–1707.

[2] G.B.D.C.o.D. Collaborators, Global, Regional, and National Age-Sex Specific Mortality for 264 Causes of Death vol. 390, 2017, pp. 1151–1210, 1980-2016: a systematic analysis for the Global Burden of Disease Study 2016, Lancet, 10100.

[3] M. Gheorghiade, G. Sopko, L. De Luca, E.J. Velazquez, J.D. Parker, P.F. Binkley, Z. Sadowski, K.S. Golba, D.L. Prior, J.L. Rouleau, R.O. Bonow, Navigating the crossroads of coronary artery disease and heart failure, Circulation 114 (11) (2006) 1202–1213.

[4] P.A. Heidenreich, N.M. Albert, L.A. Allen, D.A. Bluemke, J. Butler, G.C. Fonarow, J. S. Ikonomidis, O. Khavjou, M.A. Konstam, T.M. Maddox, G. Nichol, M. Pham, I. L. Pina, J.G. Trogdon C, American heart association advocacy coordinating, T. Council on arteriosclerosis, B. Vascular, R. Council on cardiovascular, intervention, C. Council on clinical, E. Council on, prevention, C. Stroke, forecasting the impact of heart failure in the United States: a policy statement from the American heart association, Circ Heart Fail 6 (3) (2013) 606–619.

[5] A.S. Bhatt, A.P. Ambrosy, E.J. Velazquez, Adverse remodeling and reverse remodeling after myocardial infarction, Curr. Cardiol. Rep. 19 (8) (2017) 71.

[6] S. Huang, N.G. Frangogiannis, Anti-inflammatory therapies in myocardial infarction: failures, hopes and challenges, Br. J. Pharmacol. 175 (9) (2018) 1377–1400.

[7] Y. Ling, L. Bao, W. Yang, Y. Chen, Q. Gao, Minimally invasive direct coronary artery bypass grafting with an improved rib spreader and a new-shaped cardiac stabilizer: results of 200 consecutive cases in a single institution, BMC Cardiovasc. Disord. 16 (2016) 42.

[8] Y. Ling, X. Liu, Y. Chen, S. Chen, X. Jin, S. Dong, F. Wan, One center experience in China, Int. J. Clin. Exp. Med. 8 (11) (2015) 21477–21481.

[9] A. Trounson, C. McDonald, Stem cell therapies in clinical trials: progress and challenges, Cell Stem Cell 17 (1) (2015) 11–22.

[10] V.Y. Suncion, E. Ghersin, J.E. Fishman, J.P. Zambrano, V. Karantalis, N. Mandel, K. H. Nelson, G. Gerstenblith, D.L. DiFede Velazquez, E. Breton, K. Sitammagari, I. H. Schulman, S.N. Taldone, A.R. Williams, C. Sanina, P.V. Johnston, J. Brinker, P. Altman, M. Mushtaq, B. Trachtenberg, A.M. Mendizabal, M. Tracy, J. Da Silva, I. K. McNiece, A.C. Lardo, R.T. George, J.M. Hare, A.W. Heldman, Does transendocardial injection of mesenchymal stem cells improve myocardial function locally or globally?: an analysis from the Percutaneous Stem Cell Injection Delivery Effects on Neomyogenesis (POSEIDON) randomized trial, Circ. Res. 114 (8) (2014) 1292–1301.

[11] K. Chen, Y. Huang, R. Singh, Z.Z. Wang, Arrhythmogenic risks of stem cell replacement therapy for cardiovascular diseases, J. Cell. Physiol. 235 (9) (2020 Sep) 6257–6267.

[12] Y. Shiba, T. Gomibuchi, T. Seto, Y. Wada, H. Ichimura, Y. Tanaka, T. Ogasawara, K. Okada, N. Shiba, K. Sakamoto, D. Ido, T. Shiina, M. Ohkura, J. Nakai, N. Uno, Y. Kazuki, M. Oshimura, I. Minami, U. Ikeda, Allogeneic transplantation of iPS cell-derived cardiomyocytes regenerates primate hearts, Nature 538 (7625) (2016) 388–391.

[13] S. Okano, Y. Shiba, Therapeutic potential of pluripotent stem cells for cardiac repair after myocardial infarction, Biol. Pharm. Bull. 42 (4) (2019) 524–530.

[14] V.B. Fernandez Vallone, M.A. Romaniuk, H. Choi, V. Labovsky, J. Otaegui, N. A. Chasseing, Mesenchymal stem cells and their use in therapy: what has been achieved? Differentiation 85 (1–2) (2013) 1–10.

[15] G.P. Fadini, M. Miorin, M. Facco, S. Bonamico, I. Baesso, F. Grego, M. Menegolo, S. V. de Kreutzenberg, A. Tiengo, C. Agostini, A. Avogaro, Circulating endothelial progenitor cells are reduced in peripheral vascular complications of type 2 diabetes mellitus, J. Am. Coll. Cardiol. 45 (9) (2005) 1449–1457.

[16] C. Heiss, S. Keymel, U. Niesler, J. Ziemann, M. Kelm, C. Kalka, Impaired progenitor cell activity in age-related endothelial dysfunction, J. Am. Coll. Cardiol. 45 (9) (2005) 1441–1448.

[17] S. Sharma, R. Mishra, G.E. Bigham, B. Wehman, M.M. Khan, H. Xu, P. Saha, Y. A. Goo, S.R. Datla, L. Chen, M.E. Tulapurkar, B.S. Taylor, P. Yang, S. Karathanasis, D.R. Goodlett, S. Kaushal, A deep proteome analysis identifies the complete secretome as the functional unit of human cardiac progenitor cells, Circ. Res. 120 (5) (2017) 816–834.

[18] T. Li, M. Xia, Y. Gao, Y. Chen, Y. Xu, Human umbilical cord mesenchymal stem cells: an overview of their potential in cell-based therapy, Expet Opin. Biol. Ther. 15 (9) (2015) 1293–1306.

[19] L.R. Gao, Y. Chen, N.K. Zhang, X.L. Yang, H.L. Liu, Z.G. Wang, X.Y. Yan, Y. Wang, Z.M. Zhu, T.C. Li, L.H. Wang, H.Y. Chen, Y.D. Chen, C.L. Huang, P. Qu, C. Yao, B. Wang, G.H. Chen, Z.M. Wang, Z.Y. Xu, J. Bai, D. Lu, Y.H. Shen, F. Guo, M.Y. Liu,

Y. Yang, Y.C. Ding, Y. Yang, H.T. Tian, Q.A. Ding, L.N. Li, X.C. Yang, X. Hu, Intracoronary infusion of Wharton's jelly-derived mesenchymal stem cells in acute myocardial infarction: double-blind, randomized controlled trial, BMC Med. 13 (2015) 162.
[20] T. Shimizu, M. Yamato, T. Akutsu, T. Shibata, Y. Isoi, A. Kikuchi, M. Umezu, T. Okano, Electrically communicating three-dimensional cardiac tissue mimic fabricated by layered cultured cardiomyocyte sheets, J. Biomed. Mater. Res. 60 (1) (2002) 110–117.
[21] J. Yang, M. Yamato, T. Shimizu, H. Sekine, K. Ohashi, M. Kanzaki, T. Ohki, K. Nishida, T. Okano, Reconstruction of functional tissues with cell sheet engineering, Biomaterials 28 (34) (2007) 5033–5043.
[22] R. Guo, M. Morimatsu, T. Feng, F. Lan, D. Chang, F. Wan, Y. Ling, Stem cell-derived cell sheet transplantation for heart tissue repair in myocardial infarction, Stem Cell Res. Ther. 11 (1) (2020) 19.
[23] T. Shimizu, H. Sekine, Y. Isoi, M. Yamato, A. Kikuchi, T. Okano, Long-term survival and growth of pulsatile myocardial tissue grafts engineered by the layering of cardiomyocyte sheets, Tissue Eng. 12 (3) (2006) 499–507.
[24] Y. Haraguchi, T. Shimizu, M. Yamato, T. Okano, Regenerative therapies using cell sheet-based tissue engineering for cardiac disease, Cardiol. Res. Pract. 2011 (2011) 845170.
[25] Y. Sawa, S. Miyagawa, Present and future perspectives on cell sheet-based myocardial regeneration therapy, BioMed Res. Int. 2013 (2013) 583912.
[26] Y. Miyahara, N. Nagaya, M. Kataoka, B. Yanagawa, K. Tanaka, H. Hao, K. Ishino, H. Ishida, T. Shimizu, K. Kangawa, S. Sano, T. Okano, S. Kitamura, H. Mori, Monolayered mesenchymal stem cells repair scarred myocardium after myocardial infarction, Nat. Med. 12 (4) (2006) 459–465.
[27] H. Okura, A. Matsuyama, C.M. Lee, A. Saga, A. Kakuta-Yamamoto, A. Nagao, N. Sougawa, N. Sekiya, K. Takekita, Y. Shudo, S. Miyagawa, H. Komoda, T. Okano, Y. Sawa, Cardiomyoblast-like cells differentiated from human adipose tissue-derived mesenchymal stem cells improve left ventricular dysfunction and survival in a rat myocardial infarction model, Tissue Eng. C Methods 16 (3) (2010) 417–425.
[28] N. Sekiya, G. Matsumiya, S. Miyagawa, A. Saito, T. Shimizu, T. Okano, N. Kawaguchi, N. Matsuura, Y. Sawa, Layered implantation of myoblast sheets attenuates adverse cardiac remodeling of the infarcted heart, J. Thorac. Cardiovasc. Surg. 138 (4) (2009) 985–993.
[29] D. Zhang, W. Huang, B. Dai, T. Zhao, A. Ashraf, R.W. Millard, M. Ashraf, Y. Wang, Genetically manipulated progenitor cell sheet with diprotin A improves myocardial function and repair of infarcted hearts, Am. J. Physiol. Heart Circ. Physiol. 299 (5) (2010) H1339–H1347.
[30] Y. Sawa, S. Miyagawa, T. Sakaguchi, T. Fujita, A. Matsuyama, A. Saito, T. Shimizu, T. Okano, Tissue engineered myoblast sheets improved cardiac function sufficiently to discontinue LVAS in a patient with DCM: report of a case, Surg. Today 42 (2) (2012) 181–184.
[31] S. Miyagawa, K. Domae, Y. Yoshikawa, S. Fukushima, T. Nakamura, A. Saito, Y. Sakata, S. Hamada, K. Toda, K. Pak, M. Takeuchi, Y. Sawa, Phase I clinical trial of autologous stem cell-sheet transplantation therapy for treating cardiomyopathy, J Am Heart Assoc 6 (4) (2017).
[32] Y. Yoshikawa, S. Miyagawa, K. Toda, A. Saito, Y. Sakata, Y. Sawa, Myocardial regenerative therapy using a scaffold-free skeletal-muscle-derived cell sheet in patients with dilated cardiomyopathy even under a left ventricular assist device: a safety and feasibility study, Surg. Today 48 (2) (2018) 200–210.
[33] R. Yamamoto, S. Miyagawa, K. Toda, S. Kainuma, D. Yoshioka, Y. Yoshikawa, H. Hata, T. Ueno, T. Kuratani, Y. Sawa, Long-term outcome of ischemic cardiomyopathy after autologous myoblast cell-sheet implantation, Ann. Thorac. Surg. 108 (5) (2019) e303–e306.
[34] T. Shimizu, M. Yamato, A. Kikuchi, T. Okano, Two-dimensional manipulation of cardiac myocyte sheets utilizing temperature-responsive culture dishes augments the pulsatile amplitude, Tissue Eng. 7 (2) (2001) 141–151.
[35] K.L. Christman, R.J. Lee, Biomaterials for the treatment of myocardial infarction, J. Am. Coll. Cardiol. 48 (5) (2006) 907–913.
[36] P. Menasche, Cardiac cell therapy: lessons from clinical trials, J. Mol. Cell. Cardiol. 50 (2) (2011) 258–265.
[37] K. Matsuura, Y. Haraguchi, T. Shimizu, T. Okano, Cell sheet transplantation for heart tissue repair, J. Contr. Release 169 (3) (2013) 336–340.
[38] P. Menasche, Cell therapy trials for heart regeneration - lessons learned and future directions, Nat. Rev. Cardiol. 15 (11) (2018) 659–671.
[39] N. Hida, N. Nishiyama, S. Miyoshi, S. Kira, K. Segawa, T. Uyama, T. Mori, K. Miyado, Y. Ikegami, C. Cui, T. Kiyono, S. Kyo, T. Shimizu, T. Okano, M. Sakamoto, S. Ogawa, A. Umezawa, Novel cardiac precursor-like cells from human menstrual blood-derived mesenchymal cells, Stem Cell. 26 (7) (2008) 1695–1704.
[40] Y. Imanishi, S. Miyagawa, N. Maeda, S. Fukushima, S. Kitagawa-Sakakida, T. Daimon, A. Hirata, T. Shimizu, T. Okano, I. Shimomura, Y. Sawa, Induced adipocyte cell-sheet ameliorates cardiac dysfunction in a mouse myocardial infarction model: a novel drug delivery system for heart failure, Circulation 124 (11 Suppl) (2011) S10–S17.
[41] J.H. Kim, H.J. Joo, M. Kim, S.C. Choi, J.I. Lee, S.J. Hong, D.S. Lim, Transplantation of adipose-derived stem cell sheet attenuates adverse cardiac remodeling in acute myocardial infarction, Tissue Eng Part A 23 (1–2) (2017) 1–11.
[42] Y. Tanaka, B. Shirasawa, Y. Takeuchi, D. Kawamura, T. Nakamura, M. Samura, A. Nishimoto, K. Ueno, N. Morikage, T. Hosoyama, K. Hamano, Autologous preconditioned mesenchymal stem cell sheets improve left ventricular function in a rabbit old myocardial infarction model, Am J Transl Res 8 (5) (2016) 2222–2233.
[43] J. Homma, H. Sekine, K. Matsuura, M. Yamato, T. Shimizu, Myoblast cell sheet transplantation enhances the endogenous regenerative abilities of infant hearts in rats with myocardial infarction, J Tissue Eng Regen Med 11 (6) (2017) 1897–1906.
[44] E.G. Roberts, B.L. Piekarski, K. Huang, S. Emani, J.Y. Wong, S.M. Emani, Evaluation of placental mesenchymal stem cell sheets for myocardial repair and regeneration, Tissue Eng Part A 25 (11–12) (2019) 867–877.
[45] J. Fujita, Y. Itabashi, T. Seki, S. Tohyama, Y. Tamura, M. Sano, K. Fukuda, Myocardial cell sheet therapy and cardiac function, Am. J. Physiol. Heart Circ. Physiol. 303 (10) (2012) H1169–H1182.
[46] F. Lan, J. Liu, K.H. Narsinh, S. Hu, L. Han, A.S. Lee, M. Karow, P.K. Nguyen, D. Nag, M.P. Calos, R.C. Robbins, J.C. Wu, Safe genetic modification of cardiac stem cells using a site-specific integration technique, Circulation 126 (11 Suppl 1) (2012) S20–S28.
[47] C. Trapnell, B.A. Williams, G. Pertea, A. Mortazavi, G. Kwan, M.J. van Baren, S. L. Salzberg, B.J. Wold, L. Pachter, Transcript assembly and quantification by RNA-Seq reveals unannotated transcripts and isoform switching during cell differentiation, Nat. Biotechnol. 28 (5) (2010) 511–515.
[48] X. An, J. Wang, H. Li, Z. Lu, Y. Bai, H. Xiao, Y. Zhang, Y. Song, Speckle tracking based strain analysis is sensitive for early detection of pathological cardiac hypertrophy, PloS One 11 (2) (2016), e0149155.
[49] S.D. Prabhu, N.G. Frangogiannis, The biological basis for cardiac repair after myocardial infarction: from inflammation to fibrosis, Circ. Res. 119 (1) (2016) 91–112.
[50] K. Lv, Q. Li, L. Zhang, Y. Wang, Z. Zhong, J. Zhao, X. Lin, J. Wang, K. Zhu, C. Xiao, C. Ke, S. Zhong, X. Wu, J. Chen, H. Yu, W. Zhu, X. Li, B. Wang, R. Tang, J. Wang, J. Huang, X. Hu, Incorporation of small extracellular vesicles in sodium alginate hydrogel as a novel therapeutic strategy for myocardial infarction, Theranostics 9 (24) (2019) 7403–7416.
[51] R.J. Vagnozzi, M. Maillet, M.A. Sargent, H. Khalil, A.K.Z. Johansen, J. A. Schwanekamp, A.J. York, V. Huang, M. Nahrendorf, S. Sadayappan, J. D. Molkentin, An acute immune response underlies the benefit of cardiac stem cell therapy, Nature 577 (7790) (2020) 405–409.
[52] M.W. Whitehouse, Anti-inflammatory glucocorticoid drugs: reflections after 60 years, Inflammopharmacology 19 (1) (2011) 1–19.
[53] V. Schwach, M. Gomes Fernandes, S. Maas, S. Gerhardt, R. Tsonaka, L. van der Weerd, R. Passier, C.L. Mummery, M.J. Birket, D.C.F. Salvatori, Expandable human cardiovascular progenitors from stem cells for regenerating mouse heart after myocardial infarction, Cardiovasc. Res. 116 (3) (2020) 545–553.
[54] A.E. Shafei, M.A. Ali, H.G. Ghanem, A.I. Shehata, A.A. Abdelgawad, H.R. Handal, K.A. Talaat, A.E. Ashaal, A.S. El-Shal, Mesenchymal stem cell therapy: a promising cell-based therapy for treatment of myocardial infarction, J. Gene Med. 19 (12) (2017).
[55] T. Matsuo, H. Masumoto, S. Tajima, T. Ikuno, S. Katayama, K. Minakata, T. Ikeda, K. Yamamizu, Y. Tabata, R. Sakata, J.K. Yamashita, Efficient long-term survival of cell grafts after myocardial infarction with thick viable cardiac tissue entirely from pluripotent stem cells, Sci. Rep. 5 (2015) 16842.
[56] H. Masumoto, T. Matsuo, K. Yamamizu, H. Uosaki, G. Narazaki, S. Katayama, A. Marui, T. Shimizu, T. Ikeda, T. Okano, R. Sakata, J.K. Yamashita, Pluripotent stem cell-engineered cell sheets reassembled with defined cardiovascular populations ameliorate reduction in infarct heart function through cardiomyocyte-mediated neovascularization, Stem Cell. 30 (6) (2012) 1196–1205.